Monitoring the Sky Conditions at Skinakas Observatory: II. DIMM seeing measurements

Makis Palaiologou

University of Crete, Department of Physics, Voutes University Campus, GR-70013 Heraklion, Greece

Ground-based astronomical observations are limited by atmospheric turbulence, which, to the naked eye, produces the twinkling of stars. The term **seeing** refers to the blurring of light from celestial objects caused by the atmosphere. Optical turbulence is caused by the mixing of parcels of air with different temperatures and hence density. The refractive index of air depends on its density and so turbulence at a boundary of air parcels with different temperatures creates a continuous screen of spatially and temporally varying refractive indices. The wavefront from an astronomical source can be considered flat at the top of the Earth's atmosphere (Fig. 1). As it propagates to the ground it becomes distorted by the optical turbulence which forms a limit to the precision of measurements.

The effect of optical turbulence is twofold. The first effect is to deform the wavefront passing through regions of higher refractive index. This limits the angular resolution of ground-based telescopes. The second effect is to locally focus and defocus the wavefront, which results in spatial intensity fluctuations, or speckles, in the pupil plane of a telescope, a phenomenon known as **scintillation**. It is the higher altitude turbulence that is primarily responsible for this effect. This is different to the phase aberrations causing images to blur, which is dominated by the strongest turbulent layer, often near the ground.

Measuring seeing: Differential Image Motion Monitor

Atmospheric seeing can be determined using a Differential Image Motion Monitor (DIMM). Its working principle is based on Sarazin & Roddier (1990), and is described by Vernin & Muñoz-Tuñón (1995).

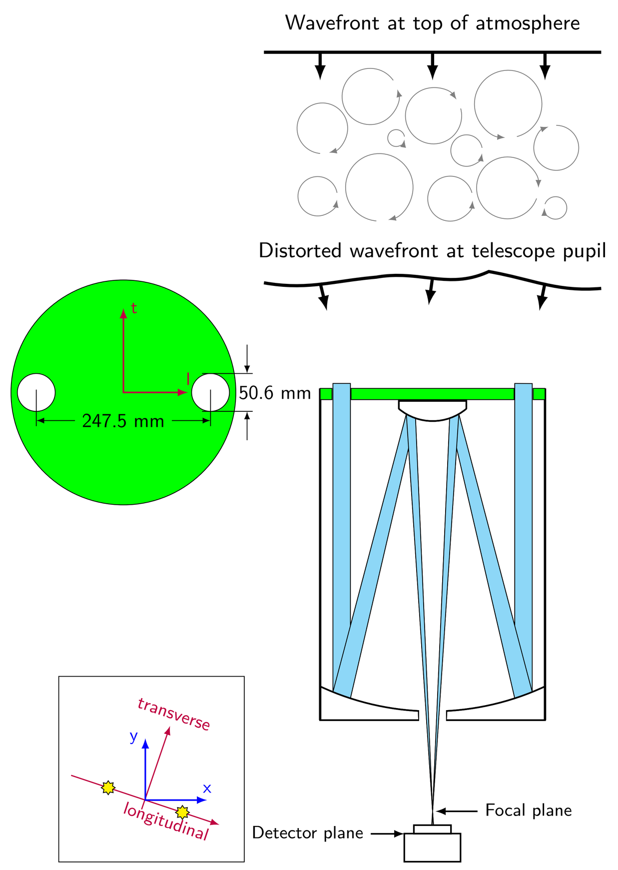

Figure 1. DIMM principle. Stellar light propagates through turbulent layers of the atmosphere to the mask apertures and forms two spots on the detector. From a set of 200 frames, the variance of the differential image positions is calculated and related to the seeing using the standard theory of optical turbulence.

The instrument is basically a 12-inch telescope with a two-pupil mask at the aperture. One of the sub-pupils has an optical wedge, so that on the focal plane two images of the observed star are formed. An intensified CCD registers the relative position of both images tens of times per second and, after at least 200 images, provides a statistical value of the seeing based on the variations of this relative position. A DIMM is not sensitive to the telescope shake and guiding errors and its field of view is usually wide, easing the pointing tolerance. These features and relative simplicity contribute to the popularity of this instrument, which became the standard for seeing measurements.

The DIMM setup used at Skinakas Observatory is based on a Meade 12" f/10 LX200 (optical diameter 305mm, focal length 3048mm) Schmidt–Cassegrain telescope, equipped with a Watec WAT-902H3 Ultimate monochrome video CCD camera for image capture. The dual star image in our case, was obtained by setting the telescope slightly out of focus, which introduces a bias (overestimated measurement). The influence of defocus on seeing measurements was studied, among others, by Tokovinin & Kornilov (2007) and Benkhaldoun & Hach (2008), who recommend to discard frames whith Strehl's ratio below 0.3. In our measurements, all exposures turned out to have a Strehl's ratio well above 0.5.

Data Acquisition

Observations took place in August **2014** (18–23) and in **2015**: June (20–21), July (10–12, 14, 18–20), August (12, 15–18), September (12, 15) and November (11–12), for a total of 25 nights. A bright star (visual mag 0–3.5) was monitored near zenith for as long as its altitude remained above 60°. Afterwards, the telescope slewed to a new bright star and the

Table 1. Characteristics of DIMM instrument

Number of pixels	720×576
Pixel scale(*)	0.″488×0.″447
Observed wavelength	500 nm
Exposure time	1–4 ms
Number of frames used for each seeing measurement	200 (every 8 sec)
Mask sub-aperture diameter (D)	50.6mm
Mask sub-aperture separation (d)	247.5mm

(*) Measured through astrometry of the open cluster M29.

sequence continued for the rest of the night, as long as weather conditions were favorable. Telescope guiding was not activated throughout the observing campaign.

After the completion of each exposure, the software detected and computed the centroid position of the two stellar images, their maximum and total intensity (to compute Strehl's ratio and the scintillation index), which were written to a text file along with the Julian date time-stamp of the exposure and relevant information concerning the target star.

Data Processing

DIMM is basically an instrument to measure the Fried parameter r_0, which is defined as the diameter of a circular area over which the RMS wavefront aberration due to passage through the atmosphere is equal to 1 radian. In practice, the parameter r_0 is the diameter of a telescope whose diffraction-limited resolving power equals the resolving power limited by the seeing. The variance of the differential image motion $\sigma_{\rm d}^2$ is related to the Fried parameter r_0 (Tokovinin, 2002)

$$\sigma_{\rm d}^2 = K\,\lambda^2\,r_0^{-5/3}\,D^{-1/3} \tag{1}$$

with λ the wavelength for which r_0 is given, D the mask sub-aperture diameter and K a proportionality constant. On the other hand, the seeing ϵ_0 is the full width at half maximum (FWHM) of the point-spread function (PSF) of a star for long exposures with a large telescope, and is computed through the equation

$$\epsilon_0 = \frac{0.98\lambda}{r_0} = 0.98\left(\frac{D}{\lambda}\right)^{1/5}\left(\frac{\sigma_{\rm d}^2}{K}\right)^{3/5} \tag{2}$$

The constant K depends on the ratio of sub-aperture separation d to their diameter D, i.e. $b = d/D$ and on the direction of image motion (*longitudinal*, along the line connecting the sub-apertures centers, or *transverse* in the orthogonal direction) (Tokovinin, 2002)

$$K_{\rm l} = 0.364(1 - 0.532\,b^{-1/3} - 0.024\,b^{-7/3})$$
$$K_{\rm t} = 0.364(1 - 0.798\,b^{-1/3} + 0.018\,b^{-7/3}) \tag{3}$$

Finally, combining Eqs. 1, 2 and 3, one gets two estimates of the seeing, corrected for the zenith distance dependence, to obtain seeing estimates referring to zenith. No further data de-debiasing (e.g. detector readout noise, exposure-time bias) was performed.

$$\epsilon_{\rm l} = 0.98\left(\frac{D}{\lambda}\right)^{1/5}\left(\frac{\sigma_{\rm l}^2}{K_{\rm l}X_{\rm eff}}\right)^{3/5},\ \epsilon_{\rm t} = 0.98\left(\frac{D}{\lambda}\right)^{1/5}\left(\frac{\sigma_{\rm t}^2}{K_{\rm t}X_{\rm eff}}\right)^{3/5} \tag{4}$$

with $X_{\rm eff}$ the effective airmass at the moment of data acquisition. The final seeing measurement is obtained by averaging the longitudinal and transverse estimates, $\epsilon_0 = (\epsilon_{\rm l} + \epsilon_{\rm t})/2$. Alternatively, Kornilov & Safonov (2011) suggest to use the "total differential image motion" variance, $\sigma_{\rm c}^2 = \sigma_{\rm l}^2 + \sigma_{\rm t}^2$, which provides a simpler interpretation of the observational data and with main advantage its weak dependence on the wind direction. In this case

$$\epsilon_0 = 0.98\left(\frac{D}{\lambda}\right)^{1/5}\left(\frac{\sigma_{\rm l}^2+\sigma_{\rm t}^2}{(K_{\rm l}+K_{\rm t})X_{\rm eff}}\right)^{3/5} \tag{5}$$

The results obtained by the two approaches do not differ by more than 1.5%. In this report we have chosen to use Eq. 5.

Our data allows us to estimate, also, the **scintillation index** s^2, defined as $s^2 = \langle\Delta I^2\rangle/\langle I\rangle^2$, with I the instantaneous light intensity received through some aperture and ΔI its fluctuation.

Results: The Ground Truth

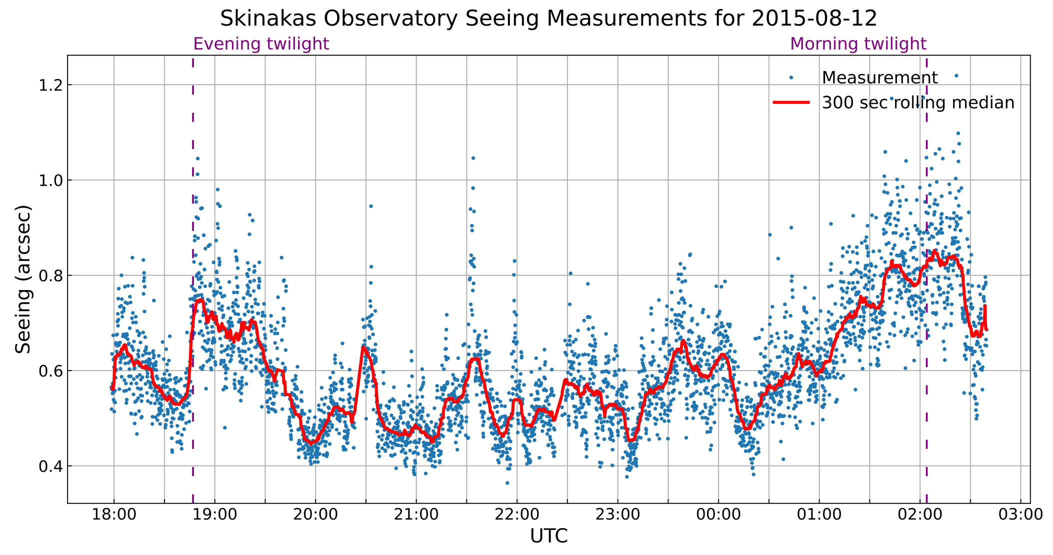

Figure 2. A **Typical** night

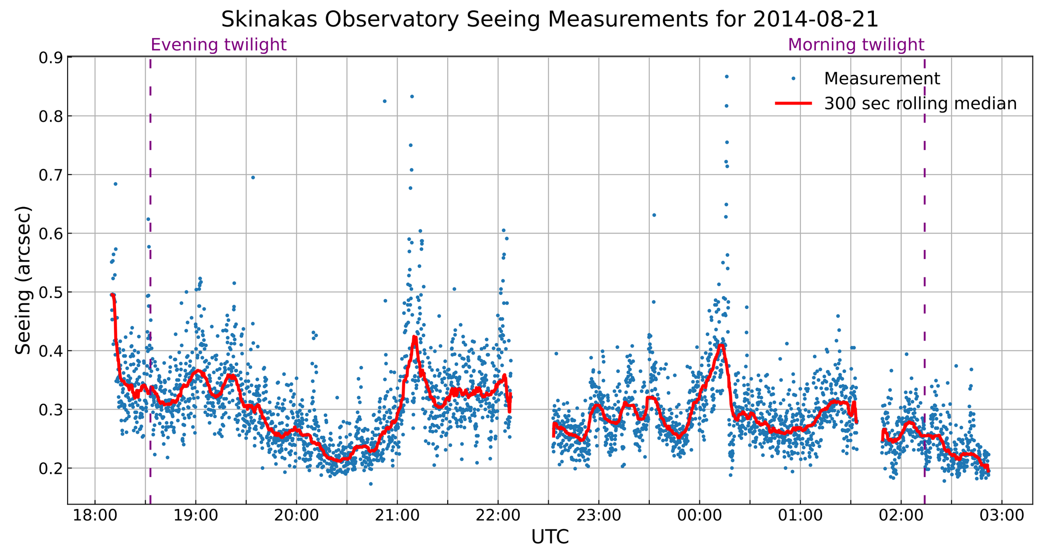

Figure 3. A **Good** night

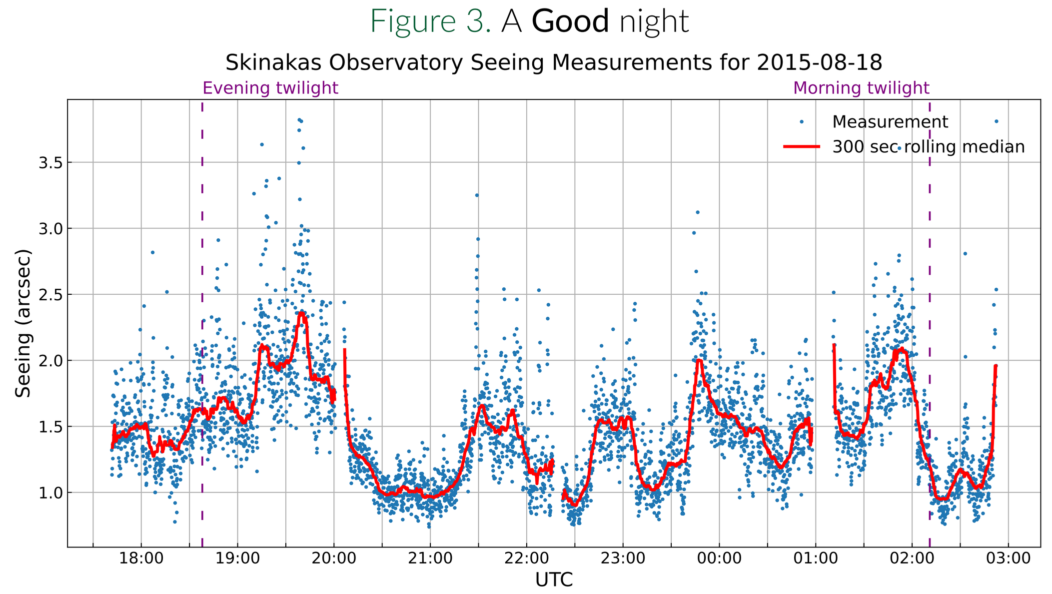

Figure 4. A **Bad** night

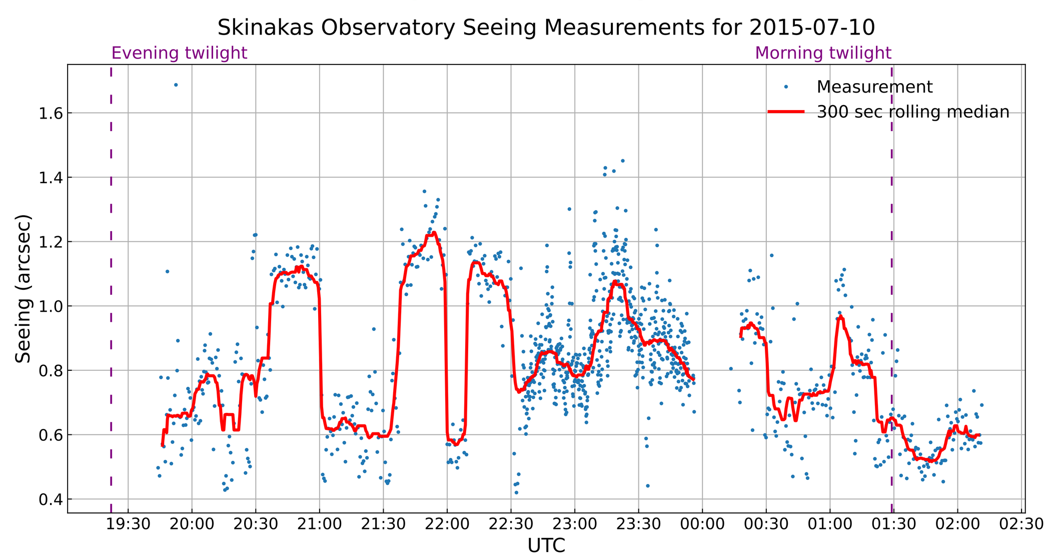

Figure 5. An **Ugly** night

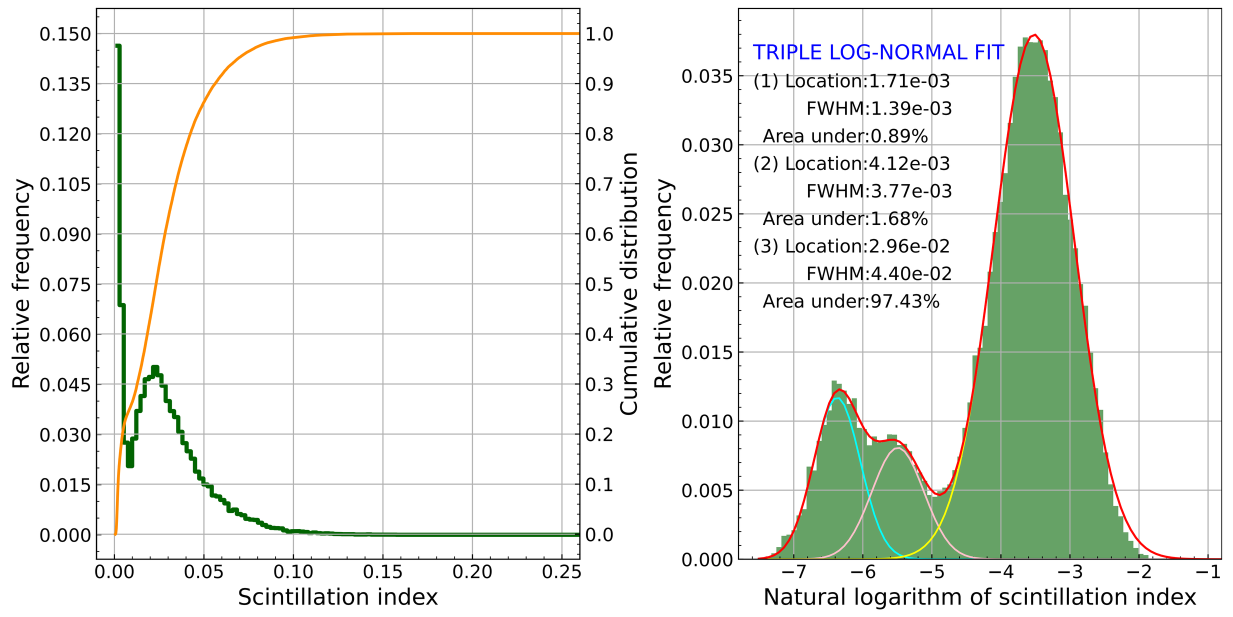

Figure 6. **Scintillation Index** statistics

Seeing Statistics

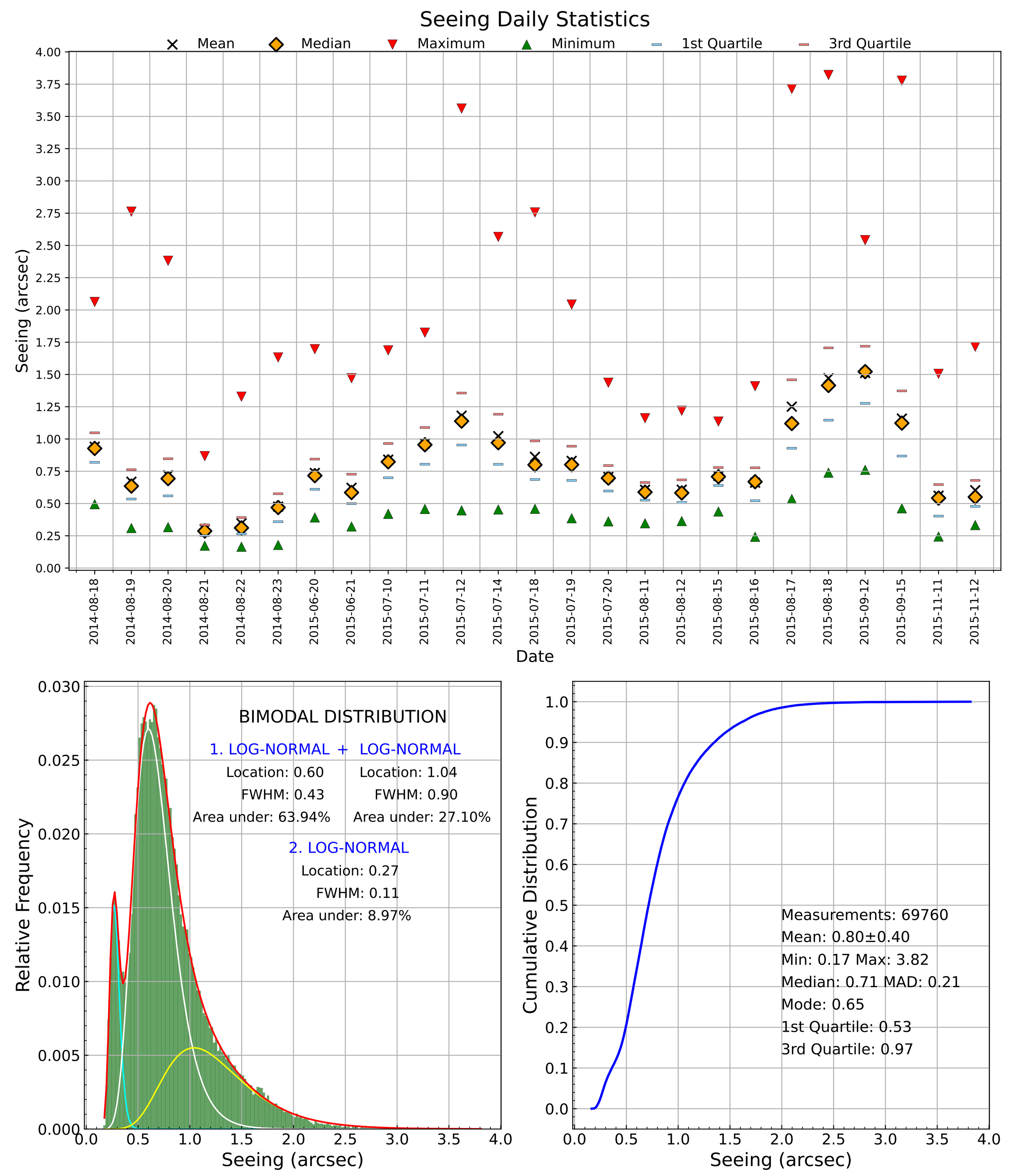

Figure 7. Seeing statistics of the entire campaign

Comparison with Other Observatories

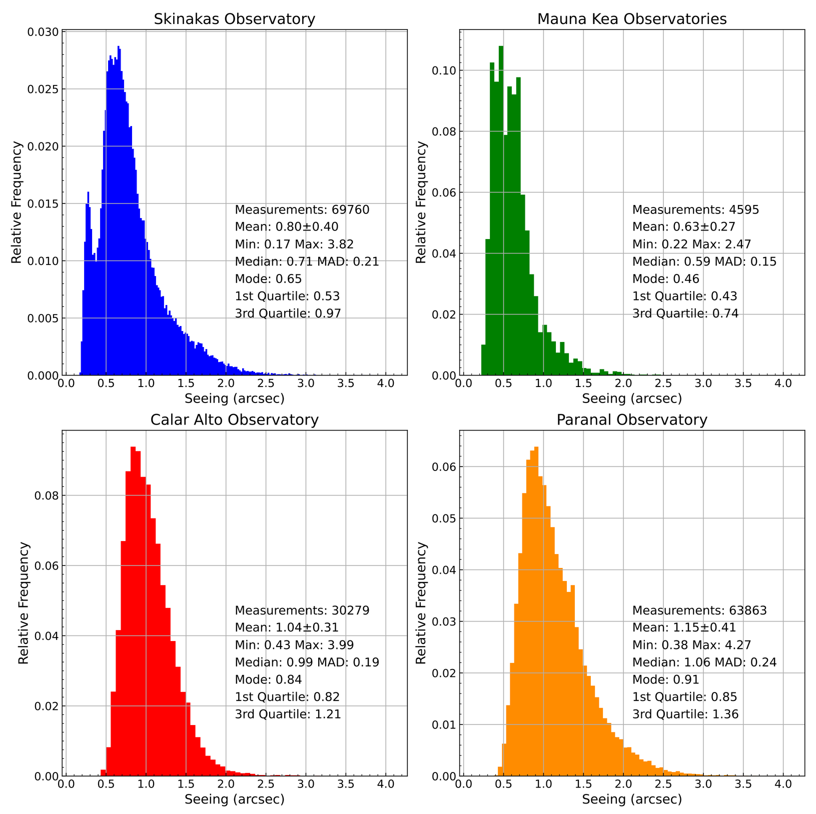

Seeing measurements were obtained from other observatories' archives, corresponding exactly to the same observing nights as in this campaign.

Figure 8. Seeing histograms between observatories

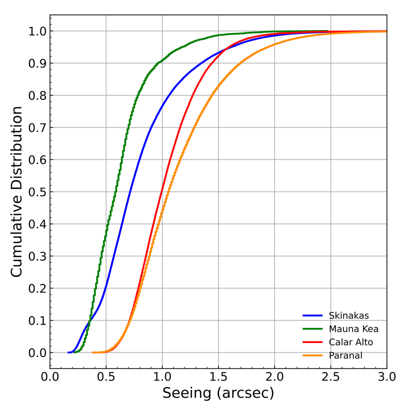

Figure 9. Cumulative seeing distributions

NOT BAD at all!

References

Benkhaldoun, Z. & Hach, Y. 2008, in Society of Photo-Optical Instrumentation Engineers (SPIE) Conference Series, Vol. 7014, Ground-based and Airborne Instrumentation for Astronomy II, ed. I. S. McLean & M. M. Casali, 70147D

Kornilov, V. & Safonov, B. 2011, MNRAS, 418, 1878

Sarazin, M. & Roddier, F. 1990, A&A, 227, 294

Tokovinin, A. 2002, PASP, 114, 1156

Tokovinin, A. & Kornilov, V. 2007, MNRAS, 381, 1179

Vernin, J. & Muñoz-Tuñón, C. 1995, PASP, 107, 265